BIOCHEMISTRY
including biophysical chemistry & molecular biology

Article

pubs.acs.org/biochemistry

Nonspecific Interactions Between *Escherichia coli* NikR and DNA Are Critical for Nickel-Activated DNA Binding

Sandra Krecisz, Michael D. Jones, and Deborah B. Zamble*

Department of Chemistry, University of Toronto, Toronto, Ontario, Canada M5S 3H6

Supporting Information

ABSTRACT: The *Escherichia coli* transcription factor NikR is responsible for nickel-mediated repression of the operon encoding the Nik uptake transporter. The crystal structure of Ni(II)-NikR bound to the *nik* operator sequence revealed that residues in the loop preceding helix α3 in the metal-binding domain, which becomes structurally ordered upon stoichiometric nickel binding, interact with the DNA backbone. Here, we show that mutating both of these residues that make the nonspecific contacts, K64 and R65, abolishes DNA binding in vitro and nickel-responsive transcriptional repression of the *nik* promoter in vivo. In contrast, mutation of Q118, which forms a bridge between R65 and a potassium site, does not impact the activities of NikR. These data support the model that the nonspecific interactions between the metal-binding domain of the protein and the DNA phosphodiester backbone are critical for the Ni(II)-responsive activity of *E. coli* NikR.

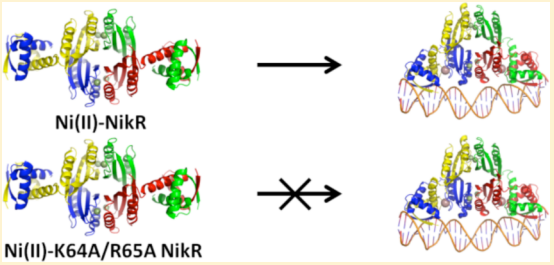

Nickel is a vital nutritional requirement for many microorganisms, but it is toxic if the intracellular levels and distribution are not strictly controlled.[1−4] As for other metals, nickel homeostasis is often governed by metal-loregulatory proteins that directly modulate the expression of genes following metal binding.[5,6] An example is the nickel-responsive NikR,[7−9] which in *Escherichia coli* (*E. coli*) represses transcription of the *nik*ABCDE operon encoding a nickel-specific importer.[10,11] The tetrameric structure of NikR (Figure 1) consists of a core of four metal-binding domains (MBDs) and two flanking ribbon−helix−helix DNA-binding domains (DBDs).[12,13] NikR binds stoichiometric nickel (4 nickel ions per tetramer) with picomolar affinity, which consequently activates DNA binding to the *nik* recognition sequence.[12,14−17] These nickel ions are located at the center of the protein and are coordinated in a square-planar geometry by H87, H89, and C95 from one MBD and H76′ from an opposing MBD.[12,13,18] There is also evidence for the binding of additional nickel ions to NikR which increase the affinity of the protein−DNA complex, although the physiological relevance of these weaker nickel sites has not yet been defined.[14,16,19−21]

The mechanism of nickel-activated DNA binding by NikR is not clear. In the crystal structure of metal-free *E. coli* NikR the two DNA-binding domains are facing in opposite directions (Figure 1), in a conformation unsuitable for simultaneous DNA binding, and the structure of the nickel-loaded protein revealed that the metal does not produce any dramatic changes in the tertiary structure.[12,13] Instead, a metal-induced stabilization of secondary structural elements of the MBD was noted. In particular, nickel reduces the disorder of helix α3, which supplies one of the metal-binding ligands, and the preceding loop (residues 63−79) (Figure 1). This observation is consistent with solution experiments demonstrating that upon loading NikR with stoichiometric nickel K64 and R65 become protected from limited tryptic proteolysis[22] and that nickel induces an increase in α-helicity in the MBD that can be observed by circular dichroism (CD) spectroscopy.[16,17,23] A functional role for the nickel-dependent ordering of this region in the center of the protein was suggested by the structure of Ni(II)-NikR bound to DNA.[13] In addition to the expected sequence-specific contacts between the DBDs and bases in the major groove of the operator half sites, there appear to be nonspecific electrostatic interactions between K64 and R65 of two of the MBDs and the DNA phosphodiester backbone (Figure 1). Furthermore, R65 is in hydrogen-bonding proximity to Q118, a residue that contributes a backbone amide carbonyl oxygen as a ligand in a potassium-binding site.[13] This potassium is bound at the interface of the MBD and DBD and is critical for NikR−DNA complex formation,[24] so Q118 could serve as a link between nickel binding and an activated DNA-binding conformation of *E. coli* NikR.

Given these structural observations, it was proposed that the allosteric mechanism of nickel-activated DNA binding by NikR includes metal-dependent organization of the α3 loops/helices. This change in the protein could promote contacts such as those between R65 and Q118, leading to potassium loading, and between the DNA phosphodiester backbone and K64 and R65. The latter nonspecific interactions could anchor NikR to the DNA, allowing the protein to initiate a one-dimensional search for its palindromic operator sequence in the *nik* promoter.[25] To test this hypothesis, we examined the activities

Received: April 19, 2012
Revised: September 11, 2012
Published: September 12, 2012

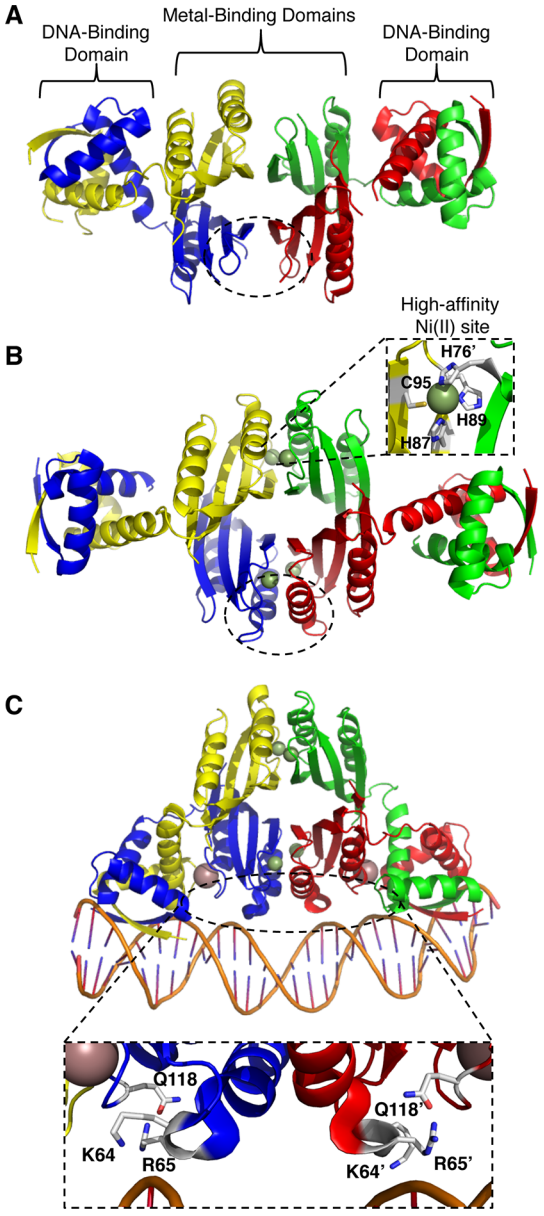

Figure 1. Crystal structures of *E. coli* NikR. (A) Metal-free NikR (PDB 1Q5V), (B) nickel-loaded NikR (PDB 2HZA), and (C) the holoprotein in a complex with its operator DNA (PDB 2HZV) are shown with each monomer in the tetramer drawn in a different color. The protein consists of a tetrameric core of MBDs and two flanking DBDs. The nickel ions (green spheres) are coordinated in a square-planar site by H87, H89, and C95 of one monomer and H76′ of an opposing monomer (shown in the inset, B). Two potassium ions (pink spheres) are bound in the DNA complex at the interface of the DBDs and the metal-binding core. Helix α3 and the preceding loop of two of the MBDs are circled and are only resolved in one of the four MBDs in the apo-NikR structure but become ordered upon stoichiometric nickel binding. K64 and R65 of two of the MBDs contact the DNA backbone (inset, C). Q118 is also shown to highlight the proximity of this residue to R65. Images generated by using Pymol.

of several *E. coli* NikR mutants both in vitro and in vivo. The results demonstrate that K64 and R65 are critical for the function of NikR but that Q118 is not, supporting the importance of the nonspecific protein−DNA interactions in the mechanism of action of this nickel-responsive transcription factor.

MATERIALS AND METHODS

Materials. Restriction endonucleases, kinases, and polymerases were obtained from New England Biolabs except where noted. The concentration of the $NiCl_2$ stock solution was confirmed by inductively coupled plasma-atomic emission spectroscopy. All other reagents were of molecular grade and purchased from Sigma-Aldrich except where noted. Primers were purchased from either Sigma-Aldrich or Integrated DNA Technologies. The plasmids pNIK103 and pPC163 were generously donated by P. Chivers (Oberlin College and Conservatory, Oberlin, OH).[15] The purified rabbit anti-NikR polyclonal antibody was purchased from CedarLane Laboratories Canada. The antibody was raised against a NikR peptide (residues 104−121) and purified using affinity chromatography with resin bearing the same peptide. All samples were prepared with Milli-Q water, 18.2 MΩ·cm resistance (Millipore), and the pH of all buffers was adjusted using either HCl or NaOH at room temperature.

Protein Mutagenesis, Expression and Purification. The single K64A, R65A, and Q118A *nikR* mutants were constructed from the pNIK103 parent plasmid[15] by using the QuickChange polymerase chain reaction (PCR) mutagenesis method (Stratagene). The K64A/R65A *nikR* mutant was constructed from the R65A pNIK103 plasmid, and the C95A *nikR* mutant was constructed from the pNIK103 parent plasmid using the Phusion PCR mutagenesis method (Thermo Fisher Scientific). The primers used are listed in Table S1. The accuracy of the mutagenesis was confirmed by DNA sequencing (ACGT or TCAG, Toronto). The proteins (WT, K64A, R65A, Q118A, and K64A/R65A) were expressed from the pNIK103 plasmid (wild-type or mutant variants) transformed into BL21(DE3)* *E. coli* cells. An overnight culture was diluted into fresh LB medium supplemented with 100 μg/mL ampicillin and grown at 37 °C for ∼2.5 h. Expression was induced for 3 h following the addition of isopropyl β-D-1-thiogalactopyranoside to a final concentration of 330 μM after A_{600} reached ∼0.6. The proteins were purified on a Ni(II)-NTA column (Qiagen), followed by anion-exchange chromatography on a MonoQ HR 10/10 column (GE Healthcare), as described previously.[17] The proteins were stored in the elution buffer (20 mM Tris, ∼300 mM NaCl, pH 7.6) at 4 °C. The C95A pNIK103 plasmid was used as a negative control for the β-galactosidase activity assays.[26] Apo-NikR was prepared by incubating NikR with 2 mM ethylenediaminetetraacetic acid (EDTA) overnight at 4 °C after the first chromatography step, and the EDTA was removed in the anion-exchange step. The lack of metal in apo-NikR was confirmed by performing 4-(2-pyridylazo)resorcinol assays.[27] The concentrations of the proteins were determined by using the absorbance at 280 nm and an extinction coefficient of 4470 M^{-1} cm^{-1} [28,29] and are reported as monomer concentrations. The proteins were analyzed by using electrospray ionization mass spectrometry (Department of Chemistry, University of Toronto); the calculated and observed masses are listed in Table S2. In addition, 5,5′-dithiobis(2-nitrobenzoic acid) colorimetric assays were performed to confirm that >95% of the protein samples existed in the reduced state.

Nickel Titrations Monitored by Electronic Absorption Spectroscopy. Nickel titrations were conducted with 25 μM protein in 20 mM Tris, pH 7.6, 100 mM KCl, and 10 mM glycine. Separate aliquots of apo-NikR were incubated with increasing concentrations of $NiCl_2$ for 1 h at room temperature

dx.doi.org/10.1021/bi300510z | *Biochemistry* 2012, 51, 7873−7879

or overnight at 4 °C. Nickel binding was monitored at 302 nm using an Agilent 8453 spectrophotometer. Nickel titrations were also conducted by adding aliquots of a $NiCl_2$ solution directly into a cuvette containing 25 μM protein. After each aliquot addition, the solution was allowed to equilibrate for 10 min, and nickel binding was monitored at 302 nm. The extinction coefficients of the protein−nickel complexes were determined by plotting the absorbance versus nickel concentration and fitting the data to a straight line. The extinction coefficients determined using both types of nickel titration methods were comparable.

Metal Competition Experiments. Ethylene glycol tetraacetic acid (EGTA) metal competition experiments were conducted with 20 μM protein in 20 mM Tris, pH 7.6, 100 mM NaCl, and 5 mM EGTA. Separate aliquots containing apo-NikR and EGTA were incubated with increasing concentrations of $NiCl_2$ overnight at 4 °C. Nickel binding was monitored at 302 nm. The fraction of nickel-bound protein was calculated using the extinction coefficients listed in Table S1. The data were analyzed as previously described[17] and fit to the Langmuir equation, $r = [\mathrm{Ni(II)}]/((K_{d(app)}) + [\mathrm{Ni(II)}])$, where r is the fraction of protein bound to nickel and $K_{d(app)}$ is the free metal concentration required for 50% binding. Data were fit using OriginPro8.

Circular Dichroism (CD) Spectroscopy. CD spectra were recorded on an Olis rapid scanning monochromator at room temperature. Approximately 10 or 40 μM protein was used in 20 mM Tris, pH 7.6, 100 mM KCl, and 10 mM glycine. Apo-NikR was incubated with stoichiometric amounts of $NiCl_2$ overnight at 4 °C. CD spectra were collected by scanning the wavelength range of 200−260 nm using a step size of 1 nm and an integration time of 2 s. Three scans were averaged for each sample, and each CD spectrum was normalized to mean residue ellipticity $[\theta]_{mre}$ (deg cm^2 dmol^{-1}) using the equation $[\theta]_{mre} = [(MM/N - 1) \times \theta]/(c \times l \times 10)$, where MM is the molecular mass of the protein in Da, N is the number of residues, θ is the measured ellipticity (degrees), c is the total protein concentration in g/mL, and l is the cell path length. The averaged spectra were smoothed by using a three period moving average. The concentrations of the apo-NikR samples were confirmed after the scans, and nickel binding was also confirmed in the holo-NikR samples by using electronic absorption spectroscopy.

Electrophoretic Mobility Shift Assays (EMSAs). EMSAs were performed with a ^{32}P-labeled 100-bp DNA probe containing the *nik* promoter that was 5′ end labeled by using T4 polynucleotide kinase and γ-^{32}P-ATP. The 100-bp DNA probe was amplified from the pPC163 plasmid using the primers 5′-CGACTGCCCATCTATTGATCCAGAACAGG-3′ and 5′-GGTAACCCCAATGGATTAAAATAGATGGCG-3′. The indicated concentrations of protein were incubated at room temperature with DNA (∼10 000−20 000 cpm) and 35 μM $NiSO_4$ in a binding buffer containing 20 mM Tris, pH 7.5, 100 mM KCl, 3 mM $MgCl_2$, 0.1% (v/v) IGEPAL, 5% glycerol, 0.1 mg/mL bovine serum albumin, and 0.1 mg/mL herring sperm DNA (Promega) for 1 h. EMSAs were conducted in the presence of excess nickel because it has been previously reported that a NikR−DNA complex is not observed in the presence of stoichiometric nickel by using this method.[14,15] The samples were loaded onto a 7% native polyacrylamide gel containing 35 μM $NiSO_4$, which had been prerun at 350 V for 30 min at 4 °C in Tris-borate (TB) running buffer (300 mM boric acid, 75 mM Tris, pH 7.6, 35 μM $NiSO_4$). The gel was run at 350 V for 3−3.5 h at 4 °C. The gel was vacuum-dried for 1 h and exposed to a phosphor screen overnight. The phosphor screen was scanned using a Pharos FX Plus Molecular Imager (BioRad), and the image was analyzed using ImageLab software (BioRad).

DNase Footprinting Assays. DNase footprinting assays were performed with a ^{32}P-labeled 156-bp DNA probe containing the *nik* promoter. A 171-bp DNA probe was amplified from the pPC163 plasmid using the primers 5′-CGACAGTGTGCAAT**CGGCCG**ATTCAGTTAAC-3′ (containing an *EagI* restriction site) and 5′-GAATCCG-TAATCATTGTCGACAGCATGGTAACCC-3′ and then 5′ end-labeled by using T4 polynucleotide kinase and γ-^{32}P-ATP. The ^{32}P-labeled 171-bp DNA probe was digested with *EagI*, and the ^{32}P-labeled 156-bp DNA probe was purified by using a 7% polyacrylamide native gel, followed by electroelution from the gel slice and ethanol precipitation. The DNase footprinting reactions were carried out in 20 μL volumes containing the indicated concentrations of protein, DNA (∼25 000−50 000 cpm), and stoichiometric or excess amounts of $NiCl_2$ in a binding buffer containing 20 mM Tris, pH 7.5, 100 mM KCl, 1 mM $MgCl_2$, and 5% (v/v) glycerol. The samples were incubated at room temperature for 30 min prior to the addition of 1 μL of 2 μg/mL DNase I (Fermentas). The Maxam−Gilbert chemical sequencing G reaction was performed by using standard protocols.[30] The samples were loaded onto an 8% denaturing polyacrylamide gel that had been prerun at 1500 V to reach a gel temperature of ∼55 °C in Tris-borate-EDTA (TBE) running buffer (89 mM boric acid, 89 mM Tris, 1 mM EDTA, pH 7.6). The gel was run at 1700 V for ∼2 h at 55 °C. The gel was vacuum-dried for 1 h and exposed to a phosphor screen overnight. The phosphor screen was scanned using a Pharos FX Plus Molecular Imager (BioRad), and the image was analyzed using ImageLab software (BioRad). Each lane was normalized to account for sample loading by comparing a reference band that was unaffected by protein binding to the corresponding band in the control sample. The degree of protection was determined by the quantification of the intensity of two bands within the binding sequence. Half-maximal binding was calculated by fitting the data to the Hill equation with a variable Hill coefficient n, $r = [\mathrm{NikR}]^n/((K_{d(app)})^n + [\mathrm{NikR}]^n)$, where r is the fraction of DNA bound to NikR and $K_{d(app)}$ is the concentration of protein required for 50% binding.[14] Data were fit using OriginPro8.

β-Galactosidase Activity Assays. β-Galactosidase activity assays were conducted using the BW25113Δ*nikr* strain of *E. coli* from the KEIO gene deletion collection (JW3446-3, *E. coli* Genetic Stock Center, Yale).[31] Minimal media was made by supplementing M9 media, pH 7.4 (1×) (Fluka Analytical), which was treated overnight with Chelex-100 (BioRad) to remove any trace metals, with 0.2% glucose, 1 mM $MgSO_4$, and 100 μM $CaCl_2$, followed by sterile filtration. The pPC181 reporter plasmid, which contains a P_{nik}-*lacZ* fusion, was made from the pPC163 plasmid using the Phusion PCR mutagenesis method (Thermo Fisher Scientific) and the primers 5′-/5Phos/ACCATGATTACGGATTCACTGGCCGTC-3′ and 5′-/5Phos/CATGGTAACCCCAATGGATTAAAATAGAT-GGAG-3′. The pPC181 plasmid differs from the pPC163 plasmid as it no longer contains the 5′ end of the *nikA* gene fused to the 5′ end of the *lacZ* gene. At least 4-fold greater expression of *lacZ* from the pPC181 plasmid over that of the pPC163 plasmid has been previously reported.[26] Cells freshly transformed with pPC181 and pNIK103 (wild-type or mutant

dx.doi.org/10.1021/bi300510z | *Biochemistry* 2012, 51, 7873−7879

variants) were grown aerobically overnight at 37 °C in LB supplemented with 50 μg/mL kanamycin (for BW25113Δ*nikr*), 100 μg/mL ampicillin (for pNIK103), and 34 μg/mL chloramphenicol (for pPC181). The cells were pelleted, washed, and divided into sterile 15 mL polypropylene tubes containing minimal media, antibiotics, and no added nickel or 1 μM $NiCl_2$. The cultures were grown anaerobically for 16 h at 37 °C in capped tubes without any headspace. After overnight growth, β-galactosidase activity assays were conducted as previously described.[32] In short, the cells were permeabilized in Z-Buffer with 0.1% sodium dodecyl sulfate (SDS) and chloroform, and β-galactosidase reactions were initiated by the addition of 4 mg/mL *o*-nitrophenyl-β-D-galactopyranoside and terminated by the addition of 1 M Na_2CO_3. Debris was removed by centrifugation, and the amount of free *o*-nitrophenol (ONP) was detected by measuring the electronic absorption at 420 nm. LacZ activity was reported in Miller units (1 Miller unit is equal to 1 nmol of ONP produced per minute). Miller units = $1000 \times [(Abs_{420} - (1.75 \times Abs_{550}))/(t \times v \times Abs_{600})]$, where Abs_{420} is the absorbance of *o*-nitrophenol, Abs_{550} is the light scatter from cell debris, which when multiplied by 1.75 is approximately the light scatter observed at 420 nm, t is the reaction time in minutes, v is the volume of cell extract assayed in milliliters, and Abs_{600} is the cell density. The experiments were repeated at least four times.

Western Blot Analysis. Crude cell lysates were prepared from the same cells that were tested in the β-galactosidase activity assays by resuspension in 20 mM Tris, pH 7.5, sonication, and centrifugation. Protein concentrations were measured by using a BCA protein assay (Pierce) with BSA as a standard, and roughly 15−25 μg of crude extract was resolved on 15% SDS−polyacrylamide gels and then transferred to poly(vinylidene difluoride) membranes (Millipore) after electrophoresis. The blots were blocked with non-fat milk for 2 h at room temperature and then probed with a 1:1000 dilution of a purified anti-NikR polyclonal antibody (1 mg/mL) overnight at 4 °C. Following incubation with the primary antibody, the blots were incubated with a secondary goat anti-rabbit antibody (BioRad) at a dilution of 1:30 000 for 1 h at room temperature. Detection and quantification of NikR were accomplished by using enhanced chemiluminescence (Pierce) and a Fluorochem 8800 gel documentation system (Alpha Innotech).

RESULTS

To further our understanding of the mechanism of action of *E. coli* NikR, we examined the ability of several mutant proteins to act as nickel-responsive transcriptional repressors in β-galactosidase activity assays. The assay employs a P_{nik}-*lacZ* reporter plasmid (pPC181) that contains the *nik*ABCDE promoter in front of the β-galactosidase gene and the pNIK103 plasmid encoding NikR.[15,26] *E. coli* BW25113Δ*nikr* cells transformed with pPC181 and pNIK103 (wild-type or mutant variants) were grown anaerobically in minimal media supplemented with or without 1 μM nickel. Although pNIK103 is constructed in a pET backbone,[15] leaky expression in the absence of chemical induction produces levels of wild-type NikR that are sufficient to repress P_{nik}-*lacZ* upon exposure of the bacteria to 1 μM nickel (Figure 2).[15,26] C95A NikR, with a mutation in the high-affinity nickel-binding site,[18] serves as a negative control.[26] Significantly higher β-galactosidase activity ($p < 0.05$) was detected in extracts of cells expressing C95A

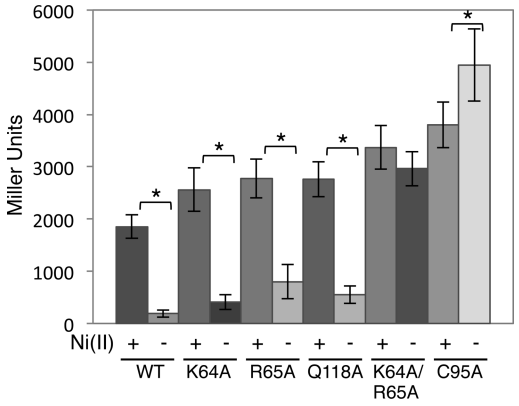

Figure 2. Transcriptional repression by wild-type and mutant NikR proteins. *E. coli* BW25113Δ*nikr* cells transformed with a P_{nik}-*lacZ* reporter plasmid and pNIK103 (encoding wild-type or mutant variants of NikR) were grown anaerobically in minimal media or media supplemented with 1 μM nickel. β-Galactosidase activity was measured in cell extracts (reported in Miller units). The data are an average of a minimum of four independent experiments ± standard deviation. A p value (from a Student's t test) of <0.05 is marked with an asterisk.

NikR grown in the absence of nickel supplementation compared to cells expressing wild-type NikR. This observation suggests that enough nickel was present in the unsupplemented media to partially activate wild-type NikR, even though precautions were taken to minimize trace nickel contamination. In support of this hypothesis, preliminary experiments demonstrated that inclusion of the nickel chelator dimethylglyoxime in the growth media of cells expressing wild-type NikR resulted in an increase in β-galactosidase activity (data not shown), although a decrease in cell growth was also noted. Finally, the increase in β-galactosidase activity observed in extracts from cells expressing C95A NikR upon nickel supplementation of the media was also observed in the absence of any pNIK103 plasmid (data not shown), suggesting that this effect is independent of NikR.

To determine the importance of K64, R65, and Q118, the effects of single alanine substitutions were examined (Figure 2). Western blot analysis was performed to confirm that the levels of protein expression of the NikR mutants are comparable (±20−40%) to that of wild-type NikR (Figure S1). All three NikR mutants, K64A, R65A, or Q118A, repress *lacZ* transcription in response to nickel supplementation, although with slightly weaker activity than wild-type NikR. This result indicates that an interaction between Q118 and R65 is not necessary for NikR to act as a nickel-activated transcriptional repressor. However, it does not rule out the importance of the electrostatic interactions with the DNA phosphodiester backbone. Given that both K64 and R65 appear to make nonspecific contacts with the DNA, it is feasible that they perform the same function such that removing only one basic residue does not hinder the activity of NikR. To test this possibility, both K64 and R65 were mutated. In contrast to the single mutations, this double mutation completely abrogated the ability of NikR to repress transcription of *lacZ* either with or without nickel supplementation.

To investigate further how the double mutation modulates NikR activity, in vitro characterization of the purified NikR mutants was also performed. Electronic absorption spectroscopy of nickel titrations demonstrated that the mutant proteins bind stoichiometric nickel tightly in a similar coordination

dx.doi.org/10.1021/bi300510z | *Biochemistry* 2012, 51, 7873−7879

Table 1. Extinction Coefficients and Nickel-Binding Affinities of NikR and the NikR Mutants[a]

	ε_{302} (M^{-1} cm^{-1})	$K_{Ni(II)}$ (M)
WT NikR	7200[b]	$(3.0 \pm 0.8) \times 10^{-12}$ [c]
K64A NikR	7500 ± 700	$(4.0 \pm 1.6) \times 10^{-12}$ [c]
R65A NikR	7100 ± 600	$(3.5 \pm 0.4) \times 10^{-12}$ [c]
Q118A NikR	7000 ± 800	$(4.5 \pm 0.9) \times 10^{-12}$ [c]
K64A/R65A NikR	6600 ± 200	$(5.1 \pm 0.2) \times 10^{-12}$ [c]
C95A NikR	0[d]	$>4 \times 10^{-5}$ [d]

[a]The extinction coefficients of the nickel−protein complexes at 302 nm are assigned to the ligand-to-metal charge transfer band of the cysteine ligand.[17,18] The data are averages of a minimum of three independent experiments ± standard deviation. [b]Previously reported.[17] [c]Estimated from competition experiments with EGTA. The data were fit to a Langmuir equation as described in the Materials and Methods section. [d]Previously reported.[18]

environment as the wild-type protein (Table 1 and data not shown), and competition experiments with EGTA revealed that the mutations did not significantly impact the affinity for nickel (Table 1). Furthermore, CD spectroscopy of the mutant proteins suggests that they all have similar overall secondary structure as wild-type NikR, with or without nickel bound (Figure S2).

To determine whether the loss of in vivo activity noted for the K64A/R65A mutant reflects the DNA-binding activity of the protein, DNase footprinting assays were performed with a 156-bp DNA probe containing the *nik* operator sequence. In addition to the double mutant, we examined the functional single mutants, K64A and R65A, in vitro along with the wild-type NikR. In the presence of stoichiometric nickel, both K64A NikR and R65A NikR protected the *nik* transcriptional start site at the same position as wild-type NikR (Figures S3 and S4). The half-maximal DNA-binding affinities were determined to be $(4 \pm 2) \times 10^{-8}$, $(1.2 \pm 0.4) \times 10^{-7}$, and $(1.2 \pm 0.5) \times 10^{-7}$ M for wild-type, K64A, and R65A Ni(II)-NikR (Figure S5), respectively, demonstrating that the single mutations do not dramatically affect the DNA-binding properties of NikR loaded with stoichiometric nickel and in agreement with the results from the in vivo activity assay. In contrast, DNase footprinting assays revealed that up to 1 μM of the double K64A/R65A NikR mutant is unable to bind to the DNA probe in the presence of stoichiometric nickel (Figure 3). Furthermore, DNase footprinting assays were also conducted with K64A/R65A NikR in the presence of excess nickel and no binding to the DNA probe was detected (Figure S6), suggesting that the DNA-binding ability of the double mutant is completely abrogated in vitro as is the activity of the protein in vivo.

Another assay that is often used to monitor the DNA-binding activity of NikR is the electrophoretic mobility shift assay (EMSA), which is performed in the presence of excess nickel.[15] As expected, DNA binding to a 100-bp DNA probe containing the *nik* promoter was not observed by K64A/R65A NikR in this assay (Figure S7). Surprisingly, DNA binding was also not detected for any of the single mutants investigated (Figure S7), in contrast to the nickel-responsive inhibition of transcription detected in the β-galactosidase assay. It is unclear why the K64A or R65A NikR−DNA complexes were not observed by EMSA, given that DNA binding was observed in the DNase footprinting experiment, although discrepancies between the two types of DNA-binding assays have been observed in the past.[14,15,24] It could be due to aggregation of the proteins in the

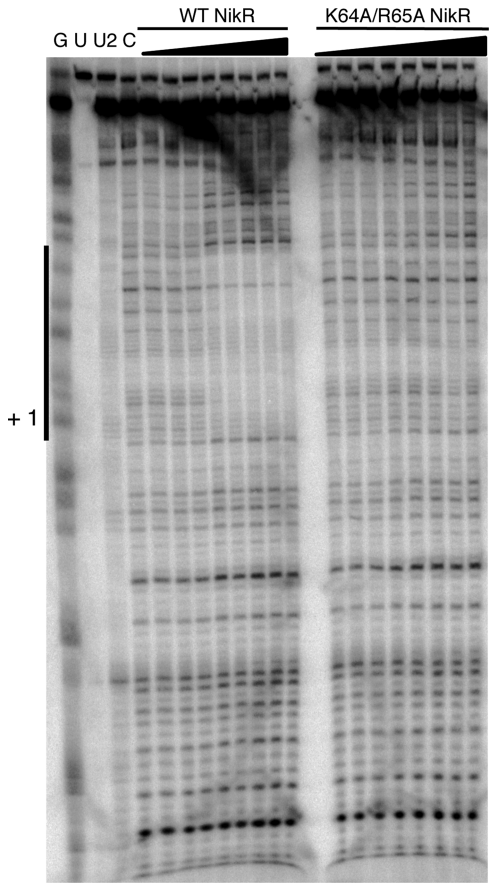

Figure 3. DNA binding by wild-type and K64A/R65A Ni(II)-NikR. WT and K64A/R65A NikR (10, 50, 100, 200, 300, 500, 800 nM and 1 μM) were incubated with a ^{32}P-labeled 156-bp DNA probe containing the *nik* recognition sequence in the presence of stoichiometric $NiCl_2$ for 1 h at room temperature prior to the addition of DNase I and analysis on an 8% denaturing polyacrylamide gel. The transcriptional start site (+1) and area of protection are indicated. Key: G, Maxam−Gilbert G reaction; U, undigested 171-bp DNA probe; U2, undigested 156-bp DNA probe; C, control DNase reaction without any NikR but with the maximum amount of nickel used. The half-maximal DNA-binding affinity of wild-type NikR from two independent experiments such as that shown was determined to be $(4 \pm 2) \times 10^{-8}$ M with a Hill coefficient of 1.6 ± 0.4.

presence of the excess metal used in the EMSA conditions, as previously reported,[14,19] but no evidence of aggregation was observed in these experiments. This observation may be related to the slight but significant alleviation of repression by the single mutants measured with the transcription assay (Figure 2), but further work is necessary to clarify the subtle impact of the single mutations.

DISCUSSION

This examination of several mutants of *E. coli* NikR elucidates aspects of the mechanism of action of the metalloregulator. At least one of the basic residues at position 64 or 65 is required for nickel-activated DNA binding in vitro and transcriptional repression in vivo, suggesting that these two residues play a critical but redundant role in the function of this metalloregulator. It is not possible to completely rule out the possibility that the double mutation disrupts the overall structure of NikR and thus impacts the behavior of the protein in a nonspecific manner. However, biochemical characterization

of the isolated mutant protein demonstrated that both the high-affinity nickel-binding activity and the overall secondary structure are preserved, suggesting that the substitutions specifically disrupt the nickel-responsive DNA-binding activity of NikR.

Despite the wealth of structural information about NikR proteins in multiple free and ligand-bound states, the mechanism of metal-activated DNA binding remains undefined. The crystal structure of the *E. coli* protein in a complex with the *nik* operator DNA revealed that both of the DBDs in a NikR tetramer must face the same side of the protein, often referred to as the down-cis conformation, in order for contacts to both half-sites in the DNA recognition sequence to occur.[13] However, it is clear from the structure of the nickel-loaded *E. coli* protein, as well as those of homologues from several other organisms, that loading with stoichiometric nickel does not force the protein to rearrange into the appropriate tertiary conformation.[12,13,33−37] Instead, DNA binding must be activated by nickel through more subtle contributions.

One impact of nickel is organization of helix α3 and the preceding loop, which is predominantly disordered in the structure of *E. coli* NikR in the apo form.[12,13] Ordering of loop/helix α3 was also observed in the structure of the MBD loaded with Cu(II),[23] which binds in a very similar square-planar site as Ni(II),[23,38] but not when the protein was loaded with noncognate zinc ions that bind with very different coordination. This metal-selective ordering of the loop/helix region in the crystal structures is consistent with the protection from limited proteolysis at this region observed for NikR loaded with nickel or copper versus other metals[22] as well as with the selectivity of metal-activated DNA binding.[14,38] Taken together, these results support the model that one mechanism by which nickel activates DNA binding is through stabilization of the loop/helix α3 structure of the MBD upon loading of the square-planar metal coordination site, resulting in a surface suitable for interacting with the DNA.

Nickel-dependent organization of these secondary structural elements in the MBD could trigger DNA binding through several mechanisms. One is by activating a hydrogen-bonding network that contains Q118. Given that the backbone carbonyl oxygen of Q118 is a ligand of the requisite potassium-binding site at the MBD−DBD interface in the DNA-bound complex,[13,24] this network could enhance potassium binding and serve as a means to communicate nickel binding to the DBDs by pulling them into the down-cis orientation. Replacing Q118 with alanine, which would disrupt the putative hydrogen bond interaction but not the potassium site, does result in a small but significant reduction in the activity of NikR in vivo, suggesting that this residue plays a minor role in the allosteric effect of nickel as previously suggested by molecular dynamics simulations.[39] However, Q118A NikR is still able to repress transcription from the *nik* promoter in response to nickel supplementation of the growth media, indicating that it is not required for the full function of the protein.

Instead, the results reported here suggest that the nonspecific electrostatic interactions between residues K64 and R65 and the DNA-phosphodiester backbone are essential for the function of NikR. It has been proposed that these nickel-activated contacts weakly anchor NikR to the DNA in a sequence-independent manner, allowing it to efficiently scan in one dimension for the *nik* recognition sequence.[25] Domain−domain motions about the flexible linker between the MBD and DBD, supported by molecular dynamics calculations,[40] would allow the protein to frequently sample the down-cis conformation and read the DNA sequence. Upon reaching the *nik* promoter, specific base contacts by DBD residues, buttressed by the bridging potassium ions, would lock the protein in its active conformation. Additional nonspecific protein interactions with the DNA phosphodiester backbone were also noted from both the DBD and the MBD,[13] and future studies will be necessary to tease out the importance of these contributions for the activity of NikR.

The conservation of this strategy for metal-induced DNA binding among NikR homologues is not clear. Several published sequence alignments of NikR homologues[34,39] reveal that although many NikR proteins have a basic residue at one or both of the positions corresponding to K64 and R65 of *E. coli* NikR,[39,41] this chemistry is not conserved. For example, nickel-dependent stabilization of the loop/helix α3 was also observed by X-ray crystallography in several subunits of NikR from *Pyrococcus horikoshii*, but this NikR homologue does not have basic residues at the equivalent positions.[34] As an alternative, the authors predicted hydrogen bonding between a backbone amide nitrogen of the protein loop and the DNA, as observed in other types of transcription factors.[42] Furthermore, in vitro analysis of NikR from *H. pylori* demonstrated that mutation of the corresponding Q76 and R77 to alanine weakened complex formation with one of its recognition sequences by several orders of magnitude,[33] although DNA binding could still be detected. In this case, R77 was linked to regulation of DNA binding by a supplemental metal site. Further research will determine whether the model of *E. coli* NikR binding to DNA can be extended to the activity of other homologues.

■ ASSOCIATED CONTENT

Supporting Information

Tables of primer sequences and mass spectrometry data, CD spectra, EMSAs, DNase footprinting assays, and Western blots. This material is available free of charge via the Internet at http://pubs.acs.org.

■ AUTHOR INFORMATION

Corresponding Author

*Phone (416) 978-3568; e-mail dzamble@chem.utoronto.ca.

Funding

This work was supported in part by funding from the Natural Sciences and Engineering Research Council (NSERC) of Canada. We also thank NSERC for financial support through a Graduate Scholarship for S.K.

Notes

The authors declare no competing financial interest.

■ ACKNOWLEDGMENTS

We thank Prof. Peter Chivers for the generous donation of the pNIK103 and pPC163 plasmids as well as members of the Zamble laboratory for critical reading of this manuscript.

■ ABBREVIATIONS

DBD, DNA-binding domain; *E. coli*, *Escherichia coli*; EGTA, ethylene glycol-bis(2-aminoethylether)-*N*,*N*,*N*′,*N*′-tetraacetic acid; EMSA, electrophoretic mobility shift assay; MBD, metal-binding domain; WT, wild-type.

REFERENCES

(1) Arita, A., and Costa, M. (2009) Epigenetics in metal carcinogenesis: nickel, arsenic, chromium and cadmium. *Metallomics 1*, 222−228.

(2) Li, Y., and Zamble, D. B. (2009) Nickel homeostasis and nickel regulation: an overview. *Chem. Rev. 109*, 4617−4643.

(3) Macomber, L., and Hausinger, R. P. (2011) Mechanisms of nickel toxicity in microorganisms. *Metallomics 3*, 1153−1162.

(4) Mulrooney, S. B., and Hausinger, R. P. (2003) Nickel uptake and utilization by microorganisms. *FEMS Microbiol. Rev. 27*, 239−261.

(5) O'Halloran, T. (1993) Transition metals in control of gene expression. *Science 261*, 715−725.

(6) Giedroc, D. P., and Arunkumar, A. I. (2007) Metal sensor proteins: nature's metalloregulated allosteric switches. *Dalton Trans.*, 3107−3120.

(7) Dosanjh, N. S., and Michel, S. L. J. (2006) Microbial nickel metalloregulation: NikRs for nickel ions. *Curr. Opin. Chem. Biol. 10*, 123−130.

(8) Iwig, J. S., and Chivers, P. T. (2010) Coordinating intracellular nickel-metal-site structure-function relationships and the NikR and RcnR repressors. *Nat. Prod. Rep. 27*, 658−667.

(9) Wang, S. C., Dias, A. V., and Zamble, D. B. (2009) The "metallo-specific" response of proteins: a perspective based on the *Escherichia coli* transcriptional regulator NikR. *Dalton Trans.*, 2459−2466.

(10) De Pina, K., Desjardin, V., Mandrand-Berthelot, M.-A., Giordano, G., and Wu, L.-F. (1999) Isolation and characterization of the *nikR* gene encoding a nickel-responsive regulator in *Escherichia coli*. *J. Bacteriol. 181*, 670−674.

(11) Navarro, C., Wu, L.-F., and Mandrand-Berthelot, M.-A. (1993) The *nik* operon of *Escherichia coli* encodes a periplasmic binding-protein-dependent transport system for nickel. *Mol. Microbiol. 9*, 1181−1191.

(12) Schreiter, E. R., Sintchak, M. D., Guo, Y., Chivers, P. T., Sauer, R. T., and Drennan, C. L. (2003) Crystal structure of the nickel-responsive transcription factor NikR. *Nat. Struct. Biol. 10*, 794−799.

(13) Schreiter, E. R., Wang, S. C., Zamble, D. B., and Drennan, C. L. (2006) NikR−operator complex structure and the mechanism of repressor activation by metal ions. *Proc. Natl. Acad. Sci. U. S. A 103*, 13676−13681.

(14) Bloom, S. L., and Zamble, D. B. (2004) Metal-selective DNA-binding response of *Escherichia coli* NikR. *Biochemistry 43*, 10029−10038.

(15) Chivers, P. T., and Sauer, R. T. (2000) Regulation of high affinity nickel uptake in bacteria. *J. Biol. Chem. 275*, 19735−19741.

(16) Chivers, P. T., and Sauer, R. T. (2002) NikR repressor: high-affinity nickel binding to the C-terminal domain regulates binding to operator DNA. *Chem. Biol. 9*, 1141−1148.

(17) Wang, S. C., Dias, A. V., Bloom, S. L., and Zamble, D. B. (2004) Selectivity of metal binding and metal-induced stability of *Escherichia coli* NikR. *Biochemistry 43*, 10018−10028.

(18) Carrington, P. E., Chivers, P. T., Al-Mjeni, F., Sauer, R. T., and Maroney, M. J. (2003) Nickel coordination is regulated by the DNA-bound state of NikR. *Nat. Struct. Biol. 10*, 126−130.

(19) Fauquant, C., Diederix, R. E., Rodrigue, A., Dian, C., Kapp, U., Terradot, L., Mandrand-Berthelot, M. A., and Michaud-Soret, I. (2006) pH dependent Ni(II) binding and aggregation of *Escherichia coli* and *Helicobacter pylori* NikR. *Biochimie 88*, 1693−1705.

(20) Phillips, C. M., Schreiter, E. R., Stultz, C. M., and Drennan, C. L. (2010) Structural basis of low-affinity nickel binding to the nickel-responsive transcription factor NikR from *Escherichia coli*. *Biochemistry 49*, 7830−7838.

(21) Wang, S. C., Li, Y., Ho, M., Bernal, M.-E., Sydor, A. M., Kagzi, W. R., and Zamble, D. B. (2010) The response of *Escherichia coli* NikR to nickel: a second nickel-binding site. *Biochemistry 49*, 6635−6645.

(22) Dias, A., and Zamble, D. (2005) Protease digestion analysis of *Escherichia coli* NikR: evidence for conformational stabilization with Ni(II). *J. Biol. Inorg. Chem. 10*, 605−612.

(23) Phillips, C. M., Schreiter, E. R., Guo, Y., Wang, S. C., Zamble, D. B., and Drennan, C. L. (2008) Structural basis of the metal specificity for nickel regulatory protein NikR. *Biochemistry 47*, 1938−1946.

(24) Wang, S. C., Li, Y., Robinson, C. V., and Zamble, D. B. (2010) Potassium is critical for the Ni(II)-responsive DNA-binding activity of *Escherichia coli* NikR. *J. Am. Chem. Soc. 132*, 1506−1507.

(25) Phillips, C. M., Stultz, C. M., and Drennan, C. L. (2010) Searching for the *nik* operon: how a ligand-responsive transcription factor hunts for its DNA binding site. *Biochemistry 49*, 7757−7763.

(26) Rowe, J. L., Starnes, G. L., and Chivers, P. T. (2005) Complex transcriptional control links NikABCDE-dependent nickel transport with hydrogenase expression in *Escherichia coli*. *J. Bacteriol. 187*, 6317−6323.

(27) Hunt, J. B., Neece, S. H., and Ginsburg, A. (1985) The use of 4-(2-pyridylazo)resorcinol in studies of zinc release from *Escherichia coli* aspartate transcarbamoylase. *Anal. Biochem. 146*, 150−157.

(28) Edelhoch, H. (1967) Spectroscopic Determination of Tryptophan and Tyrosine in Proteins. *Biochemistry 6*, 1948−1954.

(29) Pace, C. N., Vajdos, F., Fee, L., Grimsley, G., and Gray, T. (1995) How to measure and predict the molar absorption coefficient of a protein. *Protein Sci. 4*, 2411−2423.

(30) Sambrook, J., and Russell, D. W. (2001) *Molecular Cloning: A Laboratory Manual*, 3rd ed., Cold Spring Harbor Laboratory Press, New York.

(31) Baba, T., Ara, T., Hasegawa, M., Takai, Y., Okumura, Y., Baba, M., Datsenko, K. A., Tomita, M., Wanner, B. L., and Mori, H. (2006) Construction of *Escherichia coli* K-12 in-frame, single-gene knockout mutants: the Keio collection. *Mol. Syst. Biol. 2*, 1−11.

(32) Miller, J. H. (1972) *Experiments in Molecular Genetics*, Cold Spring Harbor Laboratory Press, New York.

(33) Bahlawane, C., Dian, C., Muller, C., Round, A., Fauquant, C., Schauer, K., de Reuse, H., Terradot, L., and Michaud-Soret, I. (2010) Structural and mechanistic insights into *Helicobacter pylori* NikR activation. *Nucleic Acids Res. 38*, 3106−3118.

(34) Chivers, P. T., and Tahirov, T. H. (2005) Structure of *Pyrococcus horikoshii* NikR: Nickel Sensing and Implications for the Regulation of DNA Recognition. *J. Mol. Biol. 348*, 597−607.

(35) Dian, C., Schauer, K., Kapp, U., McSweeney, S. M., Labigne, A., and Terradot, L. (2006) Structural basis of the nickel response in *Helicobacter pylori*: crystal structures of HpNikR in apo and nickel-bound states. *J. Mol. Biol. 361*, 715−730.

(36) West, A. L., Evans, S. E., Gonzalez, J. M., Carter, L. G., Tsuruta, H., Pozharski, E., and Michel, S. L. (2012) Ni(II) coordination to mixed sites modulates DNA binding of HpNikR via a long-range effect. *Proc. Natl. Acad. Sci. U. S. A. 109*, 5633−5638.

(37) West, A. L., St John, F., Lopes, P. E., MacKerell, A. D., Jr., Pozharski, E., and Michel, S. L. (2010) Holo-Ni(II)HpNikR is an asymmetric tetramer containing two different nickel-binding sites. *J. Am. Chem. Soc. 132*, 14447−14456.

(38) Leitch, S., Bradley, M. J., Rowe, J. L., Chivers, P. T., and Maroney, M. J. (2007) Nickel-specific response in the transcriptional regulator, *Escherichia coli* NikR. *J. Am. Chem. Soc. 129*, 5085−5095.

(39) Bradley, M. J., Chivers, P. T., and Baker, N. A. (2008) Molecular Dynamics Simulation of the *Escherichia coli* NikR Protein: Equilibrium Conformational Fluctuations Reveal Interdomain Allosteric Communication Pathways. *J. Mol. Biol. 378*, 1155−1173.

(40) Cui, G., and Merz, K. M., Jr. (2008) The intrinsic dynamics and function of nickel-binding regulatory protein: insights from elastic network analysis. *Biophys. J. 94*, 3769−3778.

(41) Chivers, P. T., and Sauer, R. T. (1999) NikR is a ribbon-helix-helix DNA-binding protein. *Protein Sci. 8*, 2494−2500.

(42) Ogata, K., Sato, K., and Tahirov, T. H. (2003) Eukaryotic transcriptional regulatory complexes: cooperativity from near and afar. *Curr. Opin. Struct. Biol. 13*, 40−48.